

Slicing the supercontinuum radiation generated in photonic crystal fiber using an all-fiber chirped-pulse amplification system

M. Rusu, A. B. Grudinin* and O. G. Okhotnikov

Optoelectronics Research Centre, Tampere University of Technology,
P.O. Box 692, FIN-33101, Tampere, Finland

*Fianium Ltd., UK
matei.a.rusu@orc.tut.fi

Abstract: We report on an experimental study of supercontinuum broadening in photonic crystal fiber performed by measuring the temporal behavior of spectrally-sliced radiation in different propagation regimes. The study confirms the soliton fission theory by observing the red-shifted fundamental solitons and blue-shifted nonsoliton radiation.

©2005 Optical Society of America

OCIS codes: (140.3510) Lasers, fibers; (140.4050) Mode-locked lasers; (190.4370) Nonlinear optics, fibers; (190.4380) Nonlinear optics; (320.7160) Ultrafast technology

References

1. O. G. Okhotnikov, L. Gomes, N. Xiang, T. Jouhti, and A. B. Grudinin, "Mode-locked ytterbium fiber laser tunable in the 980-1070 -nm spectral range," *Opt. Lett.* **28**, 1522 (2003).
2. O. G. Okhotnikov, T. Jouhti, J. Konttinen, S. Karirinne and M. Pessa, "1.5- μm monolithic GaInNAs semiconductor saturable-absorber mode locking of an erbium fiber laser," *Opt. Lett.* **28**, 364 (2003).
3. M. Rusu, S. Karirinne, M. Guina, A. B. Grudinin, and O. G. Okhotnikov, "Femtosecond neodymium-doped fiber laser operating in the 894-909 nm spectral range," *IEEE Photonics Technol. Lett.* **16**, 1029 (2004).
4. Fianium Ltd., *Femtopower FP1060* product datasheet, <http://www.fianium.com>
5. A. B. Rulkov, M. Y. Vyatkin, S. V. Popov, J. R. Taylor, and V. P. Gapontsev, "High brightness all-fiber generation in 525-1800 nm range with picosecond Yb pumping," *Opt. Express* **13**, 377-381 (2005), <http://www.opticsexpress.org/abstract.cfm?URI=OPEX-13-2-377>
6. K. Sakamaki, M. Nakao, M. Naganuma, and M. Izutsu, "Soliton Induced Supercontinuum Generation in Photonic Crystal Fiber," *IEEE J. Quantum Electron.* **10**, 876-883 (2004).
7. S. Coen, A. H. L. Chau, R. Leonhardt, J. D. Harvey, J. C. Knight, W. J. Wadsworth, and P. St. J. Russell, "Supercontinuum generation by stimulated Raman scattering and parametric four-wave mixing in photonic crystal fibers," *J. Opt. Soc. Am. B* **19**, 753-764 (2002).
8. J. M. Dudley, L. Provino, N. Grossard, H. Maillotte, R. S. Windeler, B. J. Eggleton, and S. Coen, "Supercontinuum generation in air-silica microstructured fibers with nanosecond and femtosecond pulse pumping," *J. Opt. Soc. Am. B* **19**, 765-771 (2002).
9. A. V. Husakou and J. Herrmann, "Supercontinuum Generation of Higher-Order Solitons by Fission in Photonic Crystal Fibers," *Phys. Rev. Lett.* **87**, 203901(1)-203901(4) (2001).
10. N. I. Nikolov, T. Sorensen, O. Bang, and A. Bjarklev, "Improving efficiency of supercontinuum generation in photonic crystal fibers by direct degenerate four-wave mixing," *J. Opt. Soc. Am. B* **20**, 2329-2337 (2003).
11. J. Herrmann, U. Griebner, N. Zhavoronkov, A. Housakou, D. Nickel, J. C. Knight, W. J. Wadsworth, P. St. J. Russell, and G. Korn, "Experimental Evidence for Supercontinuum Generation by Fission of Higher-Order Solitons in Photonic Fibers," *Phys. Rev. Lett.* **88**, 173901 1-4 (2002).
12. T. Schreiber, J. Limpert, H. Zellmer, A. Tünnermann and K. P. Hansen, "High average power supercontinuum generation in photonic crystal fibers," *Opt. Commun.* **228**, 71-78 (2003).
13. J. M. Dudley, X. Gu, L. Xu, M. Kimmel, E. Zeek, P. O'Shea, R. Trebino, S. Coen, and R. S. Windeler, "Cross-correlation frequency resolved optical gating analysis of broadband continuum generation in photonic crystal fiber: simulations and experiments," *Opt. Express* **10**, 1215-1221 (2002), <http://www.opticsexpress.org/abstract.cfm?URI=OPEX-10-21-1215>
14. K. M. Hilligsoe, H. N. Paulsen, J. Thogersen, S. R. Keiding, and J. J. Larsen, "Initial steps of supercontinuum generation in photonic crystal fibers," *J. Opt. Soc. Am. B* **20**, 1887-1893 (2003).
15. I. Zeylikovich, V. Kartazaev, and R. R. Alfano, "Spectral, temporal, and coherence properties of supercontinuum generation in microstructure fiber," *J. Opt. Soc. Am. B* **22**, 1453-1460 (2005).

16. T. Hori, N. Nishizawa, T. Goto, and M. Yoshida, "Experimental and numerical analysis of widely broadened supercontinuum generation in highly nonlinear dispersion-shifted fiber with a femtosecond pulse," *J. Opt. Soc. Am. B* **21**, 1969-1980 (2004).
 17. J. M. Dudley and S. Coen, "Numerical Simulations and Coherence Properties of Supercontinuum Generation in Photonic Crystal and Tapered Optics Fibers," *IEEE Sel. Top. Quantum Electron.* **8**, 651-659 (2002).
 18. K. Mori, H. Takara, and S. Kawanishi, "Analysis and design of supercontinuum pulse generation in single-mode optical fiber," *J. Opt. Soc. Am. B* **18**, 1780-1792 (2001).
-

1. Introduction

Supercontinuum radiation in photonic crystal fibers (PCF) has recently found exciting applications in metrology, fundamental research and medical sciences. Intensive efforts have been put into optimizing supercontinuum (SC) radiation parameters, such as spectral width, flatness and brightness, as well as developing compact all-fiber sources of ultra broadband radiation with low power consumption. Recent progress in passively mode-locked fiber lasers producing picosecond and femtosecond optical pulses stimulated the research on generation techniques and underlying mechanisms of spectral broadening in PCF. The semiconductor saturable absorber mirror (SESAM) technology has contributed greatly to the abovementioned achievements in mode-locked fiber laser. The main features of fiber-based devices – high efficiency, reliability and small footprint – make them strong competitors to the ultrafast solid-state lasers. The broad fluorescence spectrum of fiber gain media has been successfully used in tunable and ultrashort pulse sources. Recently, pulse sources operating in a wavelength range from 895 to 1560 nm were reported with neodymium, ytterbium and erbium doped fibers [1-3]. Moreover, SESAM-based mode-locked fiber lasers have reached unprecedented levels of output power and stability [4], which renders them almost ideal candidates for compact sources of supercontinuum radiation. Combined with advanced nonlinear media such as photonic crystal fibers, mode-locked fiber lasers led to significant achievements in SC generation [5]. The underlying phenomena of such a large spectral broadening are still amongst the most interesting areas in supercontinuum research. Previous studies show that self-phase modulation (SPM) alone can not produce the large spectral broadening observed at low powers in highly nonlinear photonic crystal fibers [6-8]. Moreover, detailed characterization of the supercontinuum shows that the formation of ultra-broadband spectra cannot arise solely from an interplay between SPM and four-wave mixing (FWM). Recent theories describe supercontinuum radiation as an effect of a much more complex process of soliton fission [9], assisted by SPM and FWM [10]. Further theoretical and experimental work provided evidence of soliton fission during supercontinuum generation [11-13]. It should be emphasized, however, that self-phase modulation and four-wave mixing play a substantial role in the formation and evolution of supercontinuum radiation [10], as the two phenomena act cooperatively with soliton fission to provide significant broadening of the initial pump laser spectrum [14]. Particularly, the final shape of the supercontinuum radiation spectrum is determined by a set of cascaded phenomena (SPM, FWM, soliton fission), whose contribution to the supercontinuum generation process is weighed by several system parameters, like input pulse power and duration, fiber group velocity dispersion (GVD), and fiber nonlinearity.

Temporal evolution of optical pulses within the supercontinuum spectrum gives an essential knowledge for understanding the supercontinuum formation from a relatively narrow-bandwidth pump radiation and constitutes a valuable starting point for optimizing the parameters of nonlinear media used in practical supercontinuum generators. Prior research on spectro-temporal shape of supercontinuum pulses was carried out using complex interferometric systems [15-16] and provided useful information concerning supercontinuum radiation coherence and temporal evolution. An experimental investigation of temporal shape of supercontinuum pulses in normal and anomalous dispersion regimes of the nonlinear medium is meaningful, as it clearly identifies the nature of light pulses within the

supercontinuum radiation, confirming that soliton fission assisted by SPM and FWM is the basis of supercontinuum broadening in PCF. In this paper, we demonstrate a simple scheme to characterize the temporal evolution of supercontinuum light pulses. The experimental setup employs a broadband optical filter to slice various spectral regions of a supercontinuum and a SHG autocorrelator to perform subsequent temporal shape analysis. Evidence of soliton fission-driven supercontinuum is found, along with traces of the phenomena that initiate spectral broadening.

2. Experimental setup

The setup used in the experiment is shown in Fig. 1.

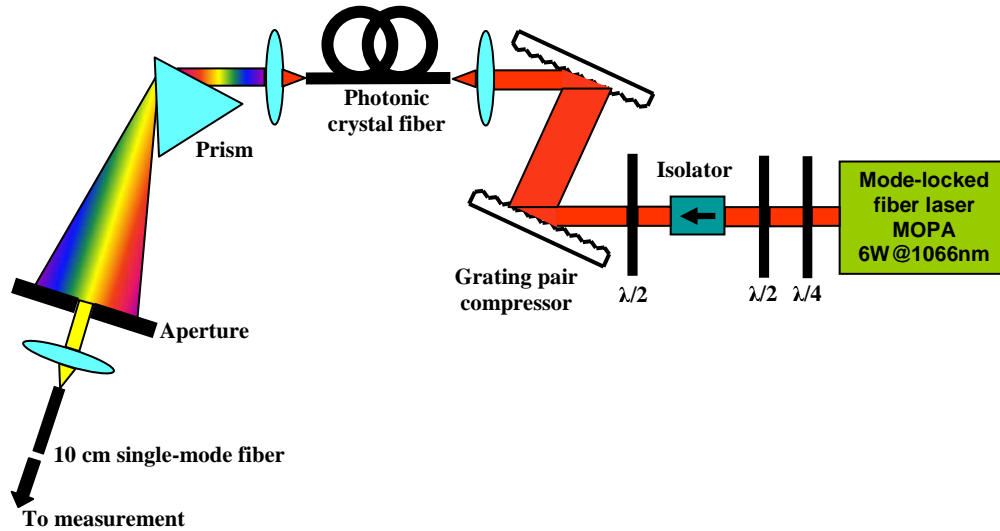


Fig. 1. Supercontinuum slicing setup with fiber MOPA pump source. MOPA: master oscillator and power amplifier

The laser source is an ytterbium (Yb) fiber-laser, mode-locked by a semiconductor saturable absorber mirror (SESAM) followed by a large mode-area (LMA) Yb-double clad fiber amplifier to boost the power. The master oscillator – power amplifier (MOPA) system produced up to 6 W of average power with 3 ps pulses at a repetition rate of 100 MHz. Figure 2 reveals the spectral characteristic of the laser output at full power and the corresponding autocorrelation trace. For optimal supercontinuum generation, the wavelength of the pump laser was set to 1066 nm, close to the zero-dispersion wavelength of the nonlinear fiber.

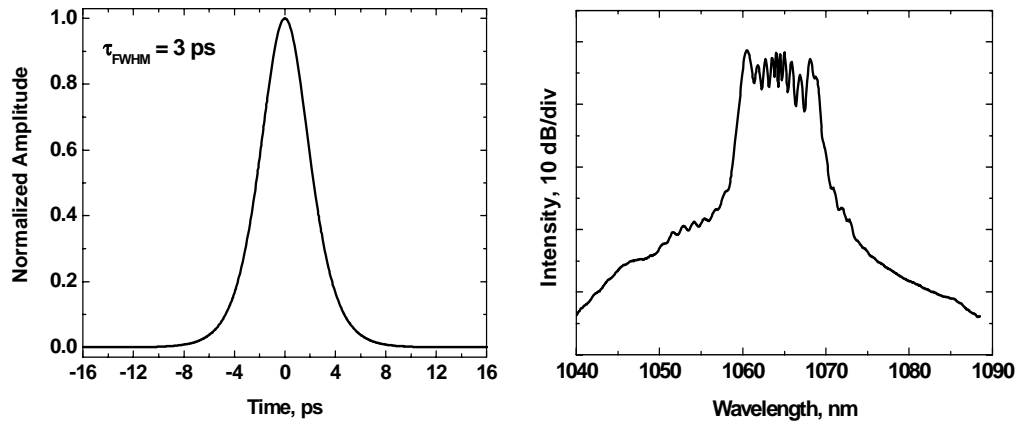


Fig. 2. Intensity autocorrelation and spectrum of the fiber source taken at full power.

Owing to nonlinearities in the amplifier fiber, the output pulses were up-chirped, which allowed for subsequent pulse compression in a diffractive grating pair exhibiting negative dispersion. The pulses emerging from the laser source are passed through a set of quarter- and half-wave plates which provide polarization corrections to the beam. A free-space optical isolator was employed to avoid back-reflections to the high-power amplifier which may adversely influence the system output power and spectrum. An additional half-wave plate aligns the polarization state of the light emerging from the isolator to ensure low-loss transmission through the grating pair pulse compressor. The grating pair removes the spectral chirp, resulting in the temporal compression of the pulse. Optimized group velocity dispersion of the grating pair yields a pulse width of 430 fs. This arrangement is known as chirped-pulse amplification (CPA) technique. The de-chirped pulse width and spectrum are shown in Fig. 3. Owing to very low nonlinearity, the grating pair compressor introduces only a minor distortion to the pulse spectrum.

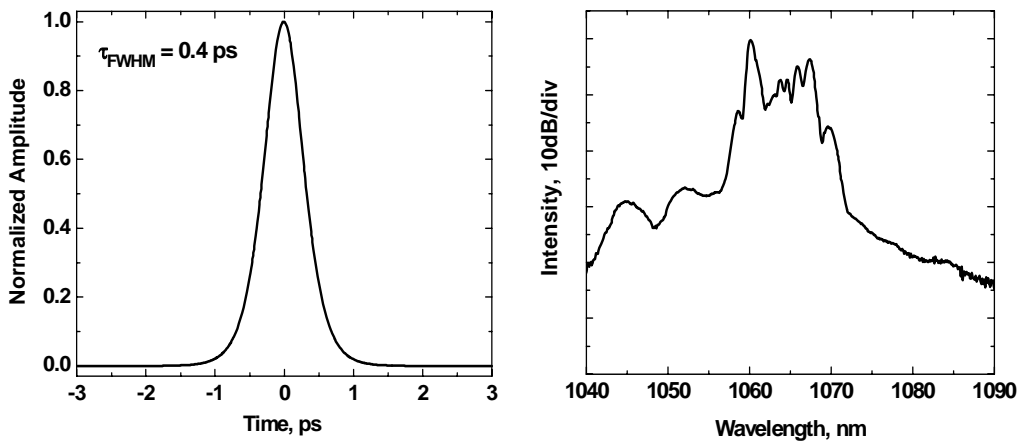


Fig. 3. Compressed pulse autocorrelation and spectrum.

The average power after the grating compressor was 2.4 W. When driven close to maximum power, the laser output beam becomes randomly polarized, which creates additional losses in the grating compressor and optical isolator.

3. Experimental results

Firstly, the compressed pulses in Fig. 3 are coupled into a 15 m span of highly nonlinear fiber (Crystal Fibre NL-5.0-1065) with the zero dispersion wavelength around 1065 nm, and dispersion characteristic shown as inset in Fig. 4. The fiber transmission efficiency was 50% (accounting for lens coupling and fiber transmission losses), resulting in an average power of 1.2 W at the output of the fiber. Strong nonlinear interactions in the fiber led to the formation of broad supercontinuum radiation, presented in Fig. 4.

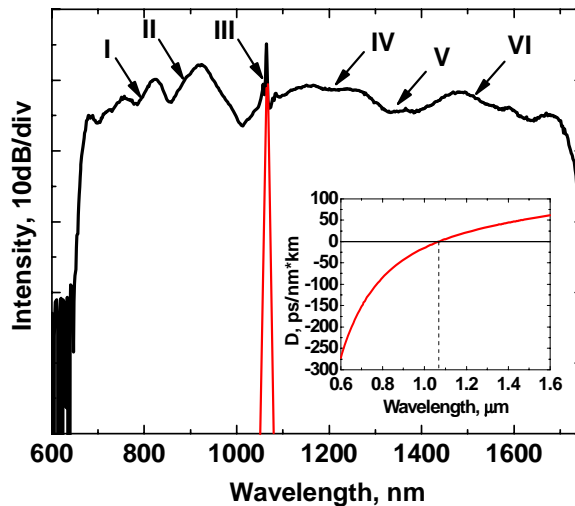


Fig. 4. Supercontinuum spectrum obtained with the setup shown in Fig. 1. Input laser spectrum at 1.06 μm is plotted with a red line. The inset shows the PCF dispersion map.

The supercontinuum generation was then investigated using pulses taken directly from the output of the power amplifier without subsequent compression in the grating pair compressor. The SC and pump spectra are illustrated in Fig. 5. Comparison of the supercontinuum spectra obtained with and without pulse compression reveals that the use of compressed pulses yielded only a minor improvement in the spectral bandwidth.

In the current system configuration, the uncompressed pulses energy was 40 nJ and their peak power was 13 kW. Following compression in the grating pair, laser pulses energy dropped to 24 nJ (as a result of losses in the compressor), whereas the peak power increased to 60 kW. Despite notable difference in the pulse characteristics, the compressed and uncompressed pulse trains produced nearly identical supercontinuum spectra. One reason behind this feature is the behavior of the pulse during the initial steps of supercontinuum generation. As shown further in the paper, upon entering the supercontinuum fiber, the pump pulse undergoes significant temporal compression attributed to an interplay between GVD and SPM [17].

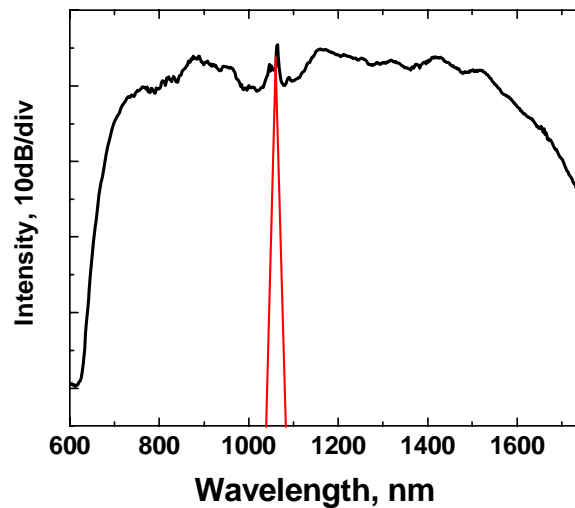


Fig. 5. Supercontinuum spectrum when uncompressed pulses are coupled into PCF (15 m of NL-5.0-1065 fiber). Input average power is 4 W, and output power is 1W. Input laser spectrum is plotted with red line.

The broad pulses with high energy are efficiently compressed inside the nonlinear fiber and reach peak power level comparable to the power of the pulses pre-compressed in the grating pair, thus leading to a comparable supercontinuum spectrum. Furthermore, assuming that the peak power is high enough, a long pulse would be converted inside the nonlinear fiber to a high order soliton, which in turn splits into a large number of fundamental solitons, resulting in a large amount of blue-shifted non-solitonic radiation emitted upon fission [9]. Owing to their relatively large peak power, the long uncompressed pulses generate large number of fundamental solitons and, consequently, a broad supercontinuum spectrum. These observations lead to a generic design guideline for supercontinuum generator sources: one should employ a source producing relatively broad pulses with high peak power. This will lead to high order solitons available for fission, and simultaneously stimulate peak power driven processes (SPM, Raman shifting, self-steepening, etc.). Therefore, practical designs should attempt a trade-off between pulse width and peak power to achieve optimal spectrum width.

To analyze temporal shape of supercontinuum pulses at different wavelengths, we performed spectrum slicing by means of a prism, as shown in Fig. 1. The prism was mounted on a motorized stage which can be precisely rotated, thus directing various wavelength components into the filtering aperture. By rotating the prism, the entire supercontinuum spectrum can be scanned. The selected spectral component is monitored with an optical spectrum analyzer, while an intensity autocorrelation trace is simultaneously taken for each selected part of the spectrum. The bandwidth of the spectral filter varied between 20 and 70 nm. To inspect the effects involved in the formation of supercontinuum, several sub-bands within the supercontinuum spectrum have been investigated. The central wavelengths of the explored sub-bands are marked in Fig. 4. The measurements of the spectrally-sliced pulses in normal and anomalous dispersion regimes confirm the soliton character of the pulses in anomalous dispersion regime and the stretched pulse character of the pulses sliced from the blue-shifted part of the spectrum, as predicted by the soliton fission theory [9]. Figure 6 shows the autocorrelations and spectra of the pulses sliced from the short-wavelength part of the supercontinuum spectrum with normal dispersion regime of propagation (indicated as I and II on Fig. 4). The peculiar shape of the autocorrelation trace is due to the non-solitonic

properties of these pulses. Since the pulses propagate in normal dispersion regime, they undergo significant broadening and overlapping leading to autocorrelation features seen in Fig. 6. The autocorrelations and optical spectra in Fig. 6(b) and 6(d) are obtained directly after the output aperture shown in Fig. 1. The spectral width of the filter was set to avoid the pulse duration being influenced by excessive spectral filtering.

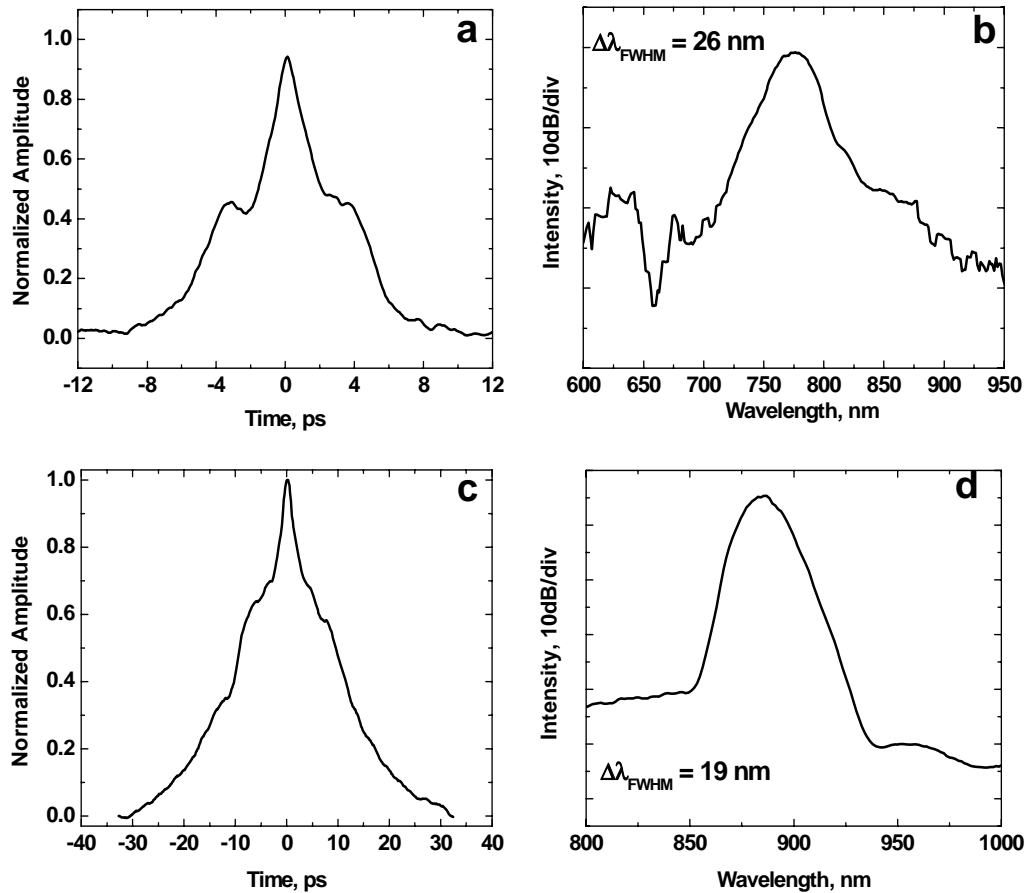


Fig. 6. Autocorrelations and spectra of the SC pulses in normal dispersion region, at 770 nm (a and b) and 880 nm (c and d).

Optical spectra and autocorrelation traces of the pulses sliced from the supercontinuum spectrum near the zero-dispersion wavelength of the nonlinear fiber are presented in Fig. 7. The spectral feature at 1065 nm originating from the residual pump is evident in the spectrum as a sharp peak (Fig. 7(b)).

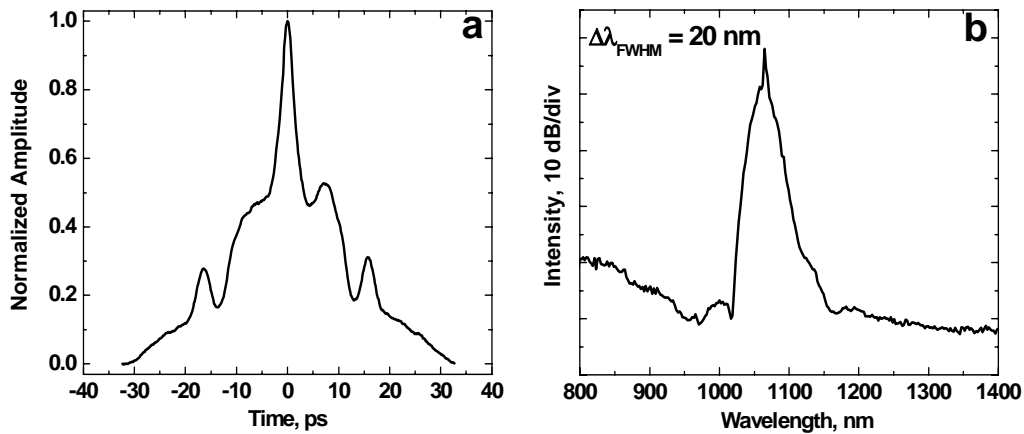


Fig. 7. Autocorrelation and spectrum of pulse sliced near zero dispersion wavelength (1065 nm)

The autocorrelation of the pump pulse shows apparent pulse breakup, which is in agreement with the theory [17]. It is worth noting that the pulse presented in Fig. 7 can be primarily regarded as a residual pump pulse left unconverted into supercontinuum radiation after propagation through the nonlinear fiber. The spike seen in the autocorrelation reveals the pulse width of 140 fs indicating that before Raman shifting, the input pulse undergoes significant compression, as described in [18]. This peak feature is ~ 3 times shorter than the initial input pulse shown in Fig. 3.

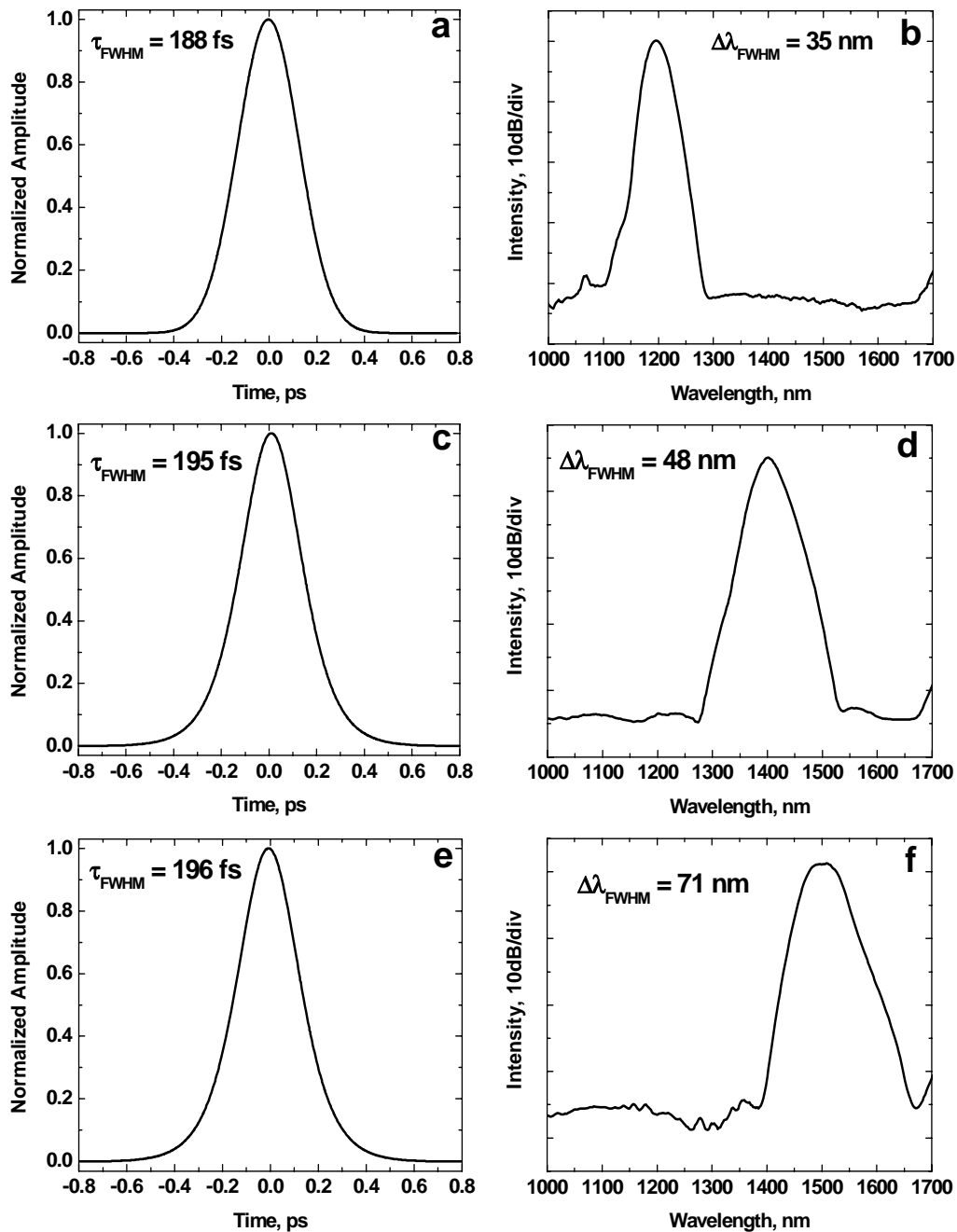


Fig. 8. Autocorrelation and spectra of pulses in anomalous dispersion regime: 1200 nm (a, b), 1400 nm (c, d), and 1500 nm (e, f).

The characteristics of the pulses in anomalous dispersion regime are shown in Figs. 8(a)-(f). The smooth, clean autocorrelations of the pulses in this regime indicate that they are steady-state solitons in agreement with the theoretical conclusions made in [9]. The soliton pulses are much shorter than the blue-shifted pulses, as inferred from Fig. 6. The sharp rise at the right

end of the spectra in Fig. 8 is a spectrum analyzer artifact. All pulse widths have been derived assuming a sech^2 pulse shape. Despite the smooth, symmetric shape of the autocorrelation traces in Fig. 8, the calculated time-bandwidth product of the measured pulses exceeds the transform-limited value for fundamental solitons. This feature is likely due to the filtering procedure that provided spectra exceeding the bandwidth of the fundamental soliton. Another interesting feature derived from Fig. 8 is that the soliton pulses in the spectral range between 1200 and 1500 nm have practically the same width despite a 3-fold change of the nonlinear fiber dispersion in the mentioned wavelength range. This could be explained by the fact that spectral shift towards longer wavelengths requires pulses with higher energy. Therefore, it is expected that long-wavelength solitons have higher energies and, consequently, shorter durations. This phenomenon is balanced by the dispersion profile of the PCF and results in similar durations of the fundamental solitons observed at different wavelengths.

The temporal stability of the pulses sliced from the supercontinuum spectrum was studied for different dispersion regimes of the photonic crystal fiber. The situation shown in Fig. 9 has been observed for any scheme of supercontinuum generation discussed above.

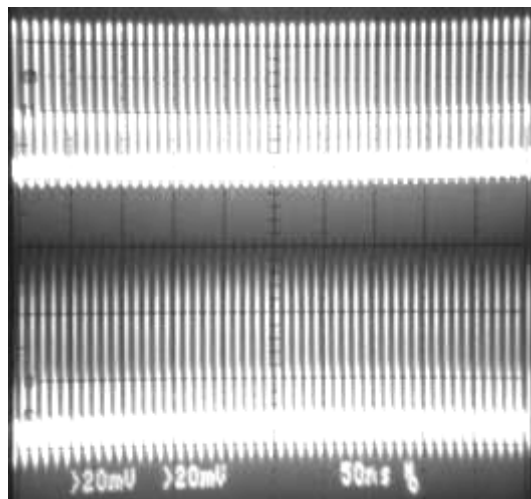


Fig. 9. Oscilloscope traces showing pulse train for soliton propagation regime (top) and normal dispersion regime (bottom).

The pulses sliced from the supercontinuum in the soliton regime can be clearly displayed on an analog scope (top trace in Fig. 9). On the contrary, the pulse train sliced at normal dispersion regime, i.e. nonsoliton radiation, exhibits significant noise visible on the output pulses. The noise appears as large pulse-to-pulse amplitude variation.

4. Conclusions

We have investigated the temporal shape of different frequency components inside supercontinuum radiation. The measurements confirm the higher-order soliton fission theory. Upon launching into the fiber, the pump pulse first experiences significant compression followed by pulse breakup. The breakup of higher-order solitons results in the formation of red-shifted fundamental solitons and blue-shifted nonsoliton radiation. The fundamental solitons with different colors propagate down the fiber at different group velocities without observable shape distortion. Due to the presence of several solitons with various frequencies, multiple blue-shifted peaks are generated leading to the formation of blue-shifted continuum. The blue-shifted pulses are longer than the soliton pulses by almost an order of magnitude and experience further severe broadening during propagation. The results provide an insight into

the fundamental mechanisms of supercontinuum generation and would be useful in designing supercontinuum sources.

Acknowledgments

The authors acknowledge the financial support of the Finnish Academy of Sciences through SUPERNAL and GEMINI projects and the EU FP-6 URANUS project.